BJP BRITISH JOURNAL OF PHARMACOLOGY

BPS BRITISH PHARMACOLOGICAL SOCIETY

British Journal of Pharmacology (2010), 159, 698–708

0007-1188/10
www.brjpharmacol.org

RESEARCH PAPER

Relevance of conserved lysine and arginine residues in transmembrane helices for the transport activity of organic anion transporting polypeptide 1B3

H Glaeser[1]*, K Mandery[1]*, H Sticht[2], MF Fromm[1] and J König[1]

[1]*Institute of Experimental and Clinical Pharmacology and Toxicology, Friedrich-Alexander-University Erlangen-Nuremberg, Erlangen, Germany, and* [2]*Division of Bioinformatics, Institute of Biochemistry, Friedrich-Alexander-University Erlangen-Nuremberg, Erlangen, Germany*

Background and purpose: Organic anion transporting polypeptide 1B3 (OATP1B3) (*SLCO1B3*) mediates the uptake of endogenous substrates (e.g. estrone-3-sulphate) and drugs (e.g. pravastatin) from blood into hepatocytes. Structure-based modelling of OATP1B3 suggested that a pore with a positive electrostatic potential contributes to the transport mechanism. Therefore, we investigated the role of conserved positively charged amino acids for OATP1B3-mediated uptake of sulphobromophthalein (BSP) and pravastatin.
Experimental approach: Residues Lys28, Lys41 and Arg580 in OATP1B3 were substituted by alanine, arginine, glutamine, glycine or lysine. Using immunofluorescence, immunoblot analysis and cellular uptake assays, the effect of these mutations on protein expression and transport activity was investigated.
Key results: Immunofluorescence revealed that all mutants were localized in the plasma membrane with partial intracellular retention of the Arg580>Ala and Arg580>Lys mutants. Lys41>Ala, Lys41>Gln, Lys41>Gly, Arg580>Gly and Arg580>Lys showed significantly reduced transport for BSP and pravastatin. Kinetic analyses of BSP transport revealed a significant reduction of V_{max} normalized to cell surface protein expression for Lys41>Ala (wild type: 190 ± 8, Lys41>Ala:16 ± 4 pmol (mg protein)$^{-1}$ min^{-1}, $P < 0.001$), whereas V_{max} of Lys41>Arg and Arg580>Lys (103 ± 8 and 123 ± 14 pmol (mg protein)$^{-1}$ min^{-1}, $P > 0.05$) did not change significantly. This suggests that the positive charges at positions 41 and 580 are important for transport activity of BSP. Structural modelling indicated that the positively charged side chain of Lys41 is flexible within the pore. The orientation of Arg580 is defined by adjacent residues Glu74 and Asn77, which was confirmed by kinetic analysis of Glu74>Ala.
Conclusions and implications: We demonstrated that the conserved positively charged amino acids Lys41 and Arg580 are pivotal to the transport activity of OATP1B3.
British Journal of Pharmacology (2010) **159,** 698–708; doi:10.1111/j.1476-5381.2009.00568.x; published online 22 January 2010

Keywords: organic anion transport; organic anion transporting polypeptide 1B3; transport activity; side chain flexibility; mutagenesis; pravastatin; sulphobromophthalein; hepatic drug transport; molecular modelling

Abbreviations: BSP, sulphobromophthalein; OATP/Oatp, organic anion transporting polypeptide; VC, vector control; WT, wild type

Introduction

Uptake and efflux transporters are recognized as crucial determinants of the absorption, distribution and elimination of drugs and endogenous compounds (Glaeser and Fromm, 2008). Members of the organic anion transporting polypeptide (OATP/Oatp) family mediate the uptake of endogenous and xenobiotic anionic compounds from the extracellular compartment into cells. The human OATP family consists of six subfamilies (OATP1–OATP6) with 11 proteins, which are expressed in various organs such as liver, intestine, kidney, heart, placenta and brain. While most OATP family members are expressed in several tissues, the expression of OATP1B1 and OATP1B3 is restricted to the liver. Both are located in the basolateral membrane of hepatocytes. Estrone-3-sulphate, estradiol-17β-glucuronide and taurocholate were identified as endogenous substrates of OATP1B3 (König *et al.*, 2000; Abe *et al.*, 2001; Nozawa *et al.*, 2004).

Correspondence: Hartmut Glaeser, Fahrstrasse 17, 91054 Erlangen, Germany.
E-mail: hartmut.glaeser@pharmakologie.med.uni-erlangen.de
*Contributed equally to this study.
Received 23 June 2009; revised 11 September 2009; accepted 27 September 2009

Furthermore, several widely prescribed drugs, such as the HMG-CoA reductase inhibitors pravastatin and rosuvastatin or the cardiac glycoside digoxin, are also substrates of OATP1B3 (Kullak-Ublick *et al.*, 2001; Ho *et al.*, 2006; Seithel *et al.*, 2007).

All OATP proteins consist of 12 transmembrane helices with a large fifth extracellular loop (Hagenbuch and Meier, 2003; Hänggi *et al.*, 2006). They have several amino acids highly conserved throughout the family, and the predicted transmembrane structure is very similar.

Several approaches have been chosen to shed more light on protein regions responsible for the transport, and to identify amino acids crucial for substrate recognition or substrate translocation. One approach identified cysteine residues in the large fifth extracellular loop between the transmembrane domains IX and X as being important for transport activity and trafficking of OATP2B1 (Hänggi *et al.*, 2006). Because all OATPs/Oatps exhibit this large loop, which contains 10 highly conserved cysteine residues (Hagenbuch and Meier, 2003; 2004), this finding could be transferable to all other OATPs. A structure-based alignment provided more detailed insights into the structure and transport mechanism of OATP1B3 (Meier-Abt *et al.*, 2005). Based on this analysis, a pore with a positive electrostatic potential and rocker-switch type of movement as mode of transport were proposed (Meier-Abt *et al.*, 2005). A pore with a positive electrostatic potential would be consistent with the transport of negatively charged anionic OATP1B3 substrates. Nevertheless, knowledge of other molecular structures, such as specific amino acids, transmembrane helices and extracellular or intracellular loops, contributing to the transport of OATPs is limited.

Therefore, we investigated the role of conserved positively charged lysine and arginine residues, which potentially line the pore, for OATP1B3-mediated sulphobromophthalein (BSP) and pravastatin uptake and generated mutants of lysine 28, lysine 41 and arginine 580. Lysine 28 and 41 are located in the predicted transmembrane helix I of OATP1B3 (Figure 1), which faces the pore according to the proposed structural model (Meier-Abt *et al.*, 2005). Arginine 580 is conserved within all human OATPs (Figure 1), and located in the predicted transmembrane helix XI. All investigated lysine and arginine residues were replaced by either alanine, glycine or with the amino acids from the complementary position of other human OATPs in order to generate a neutral charge or to simulate the situation of other OATPs respectively. Alanine was selected in addition to glycine because alanine is regarded as a stabilizing residue, whereas glycine may lead to destabilization of helical structures. In case these amino acid changes lead to a loss of activity, replacements of the positively charged lysine or arginine residues against each other should demonstrate whether the transport activity can be rescued by a positive charge of the other amino acid. In addition, structural modelling confirmed our experimental data, and by using these models we identified amino acid residues adjacent to the investigated lysine and arginine residues, which also influenced transport kinetics.

Methods

Computer-based alignment of human OATP sequences

For the identification of conserved lysine and arginine residues within the human OATPs, all 11 members of the human OATP family were aligned using the Heidelberg UNIX Sequences Analysis Resources (Senger *et al.*, 1995) based on the Wisconsin Genetics Computer Group Program Package (Devereux *et al.*, 1984).

Mutagenesis of SLCO1B3

The mutagenesis of all investigated lysine and arginine residues was performed using the QuikChange Multi Site-Directed Mutagenesis Kit (Stratagene Europe, Amsterdam, The Netherlands) according to the manufacturer's instructions. The wild-type (WT) expression plasmid pcDNA3.1/Hygro(-)-OATP1B3 containing the reference sequence NM_019844 (http://www.ncbi.nlm.nih.gov) (Cui *et al.*, 2001) was kindly provided by Professor Dietrich Keppler (DKFZ, Heidelberg, Germany). The following primers were used for the mutagenesis reactions: Gly522>Cys: 5′-gaaattactcagcacacttgtgtgaatg cccaagagataat-3′, Lys28>Ala: 5′-gacgctgcaatggattcgcgatgttctt ggcagccc-3′, Lys28>Arg: 5′-gacgctgcaatggattccggatgttcttggcag ccc-3′, Lys28>Gly: 5′-gacgctgcaatggattcgggatgttcttggcagccc -3′, Lys41>Ala: 5′-agccctgtcattcagctatattgctgcagcactaggtgga-3′,

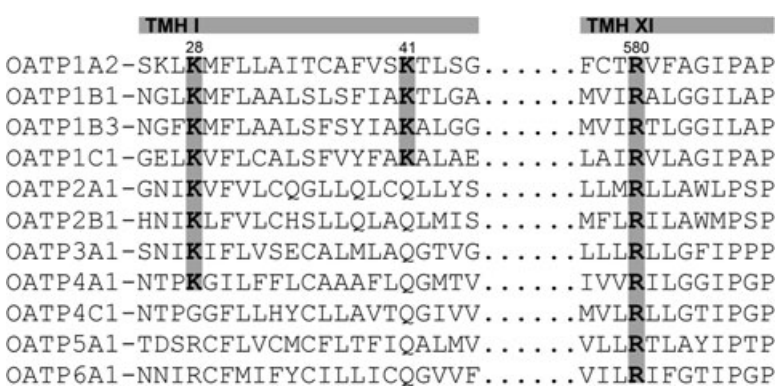

Figure 1 Partial alignment of amino acid sequences of 11 human OATPs. The alignment was performed using the Heidelberg UNIX Sequences Analysis Resources. The highlighted amino acids lysine at positions 28 and 41, and arginine at position 580 in OATP1B3 are highly conserved within the human OATP family, and are located in the predicted pore-facing transmembrane helix I (TMH I) and helix XI (TMH XI) respectively.

Lys41>Arg: 5′-agccctgtcattcagctatattgctcgagcactaggtgga-3′, Lys41>Gln: 5′-ctgtcattcagctatattgctcaagcactaggtggaatcatta-3′, Lys41>Gly: 5′-agccctgtcattcagctatattgctggagcactaggtgga-3′, Arg580>Ala: 5′-tgcaatgggtttccagtcaatggttatagcaacactaggagga at-3′, Arg580>Gly: 5′-gggtttccagtcaatggttataggaacactaggagga att-3′, Arg580>Lys: 5′-tgggtttccagtcaatggttataaaaacactaggagg aattc-3′, Glu74>Ala: 5′-tggtttaattgatggaagctttgcaattggaaa tttgcttgtgattg-3′ and Asn77>Ala: 5′-gtttaattgatggaagctttgaaatt ggagctttgcttgtgattgtatttgtaagttact-3′.

All mutagenesis products were verified by sequencing (Qiagen, Hilden and Agowa, Berlin, Germany). The Gly522>Cys mutant was used as control because the influence on the membrane localization, protein expression and uptake activity has already been described (Letschert *et al*., 2004).

Cell culture

Human embryonic kidney (HEK293) cells were cultured in minimum essential medium containing 10% heat-inactivated fetal bovine serum, 100 $U \cdot mL^{-1}$ penicillin and 100 $\mu g \cdot mL^{-1}$ streptomycin at 37°C and 5% CO_2. The cells were routinely subcultivated by trypsinization using trypsin (0.05%)–EDTA (0.02%) solution. All cell culture media supplements were obtained from Invitrogen GmbH (Karlsruhe, Germany).

Transient transfection and immunofluorescence

In order to investigate the influence of the generated mutations on the membrane localization of the OATP1B3 mutants in the transfected HEK293 cells, immunofluorescence analyses were performed. Prior to cell seeding, one circular autoclaved coverslip (diameter: 15 mm) was placed in a well of a 12-well cell culture plate, and coated with poly-D-lysine in order to increase the adherence of the cells. The HEK293 cells were seeded with a density of 300 000 per well. Twenty-four hours after seeding, the cells were transfected with 1500 ng per well of the respective expression plasmids [empty expression vector: vector control (VC), WT expression plasmid or mutant expression plasmids] using Lipofectamine 2000 (Invitrogen GmbH, Karlsruhe, Germany) according to the supplier's instructions. After a further 24 h incubation with the transfection reagent, the cells were treated with 10 mM sodium butyrate for additional 24 h (Cui *et al*., 1999) before the immunofluorescence analysis in order to increase the levels of the recombinant protein.

The immunofluorescence experiments were performed according to a previously described protocol (Lee *et al*., 2005). Briefly, the cells were washed with Tris-buffered saline (TBS; pH 7.4), and subsequently fixed in ice-cold 70% methanol for 10 min. Thereafter, the cells were permeabilized for 10 min using TBS/Triton (0.4%). The cells were blocked with 2% BSA followed by incubation with a purified rabbit antiserum against human OATP1B3 (SKT3fr2, 1:200 in blocking buffer). A Cy3-conjugated AffiniPure goat anti-rabbit IgG (Dianova, Hamburg, Germany) was used as secondary antibody (1:400 in blocking buffer). The nuclei were counterstained with the SYTOX Green dye (Invitrogen GmbH). The coverslips were inversely placed with an aqueous mounting medium (ThermoScientific, Dreieich, Germany) on a microscope slide. The fluorescence was visualized using a confocal laser scanning microscope Axiovert 100M (Carl Zeiss GmbH, Jena, Germany). The images were further processed using the Zeiss LSM Image Browser version 4.2.0.121 and Adobe Photoshop CS2 version 9.0.2.

To exclude an influence of a variability on the transfection efficiency, co-transfections of the pcDNA3.1/Hygro (-)-OATP1B3 WT or mutant plasmids with 25 ng of a β-galactosidase reference plasmid pCMVβ (Clontech, Mountain View, CA, USA) were performed. The activity of the β-galactosidase was measured as previously described (Gradhand *et al*., 2007). No significant differences between the different mutants and the WT regarding the transfection efficiency within and between different co-transfection experiments were observed (data not shown).

Transient transfection, immunoblot analysis and cell surface protein expression

The influence of the generated mutants on the respective protein amount of OATP1B3 was investigated using immunoblot analysis. HEK293 cells were seeded at a cell density of 750 000 cells per well in a poly-D-lysine-coated six-well cell culture plate. After 24 h, the cells were transfected with 4000 ng per well of the respective expression plasmids using Lipofectamine 2000 according to the supplier's instructions. After a further 24 h incubation with the transfection reagent, the cells were treated with 10 mM sodium butyrate for an additional 24 h before the immunoblot analysis. The immunoblot analysis was performed as previously described (Glaeser *et al*., 2002; 2007). Briefly, the proteins were transferred onto a nitrocellulose membrane (PROTRAN Whatman Schleicher and Schuell, A. Hartenstein GmbH, Würzburg, Germany), and incubated with a purified rabbit antiserum against human OATP1B3 (SKT3fr2, 1:300). As secondary antibody, horseradish peroxidase-labelled goat anti-rabbit Fab-fragments (Dianova) were used. The protein was visualized on autoradiography films (GE Healthcare UK Ltd, Buckinghamshire, UK) using ECL Western blotting detection reagents (GE Healthcare) and a film developer (Kodak, Stuttgart, Germany). After the detection of OATP1B3, the membranes were incubated with a Western blotting stripping buffer (Perbio Science Deutschland GmbH, Bonn, Germany) for 20 min at room temperature. Subsequently, the membranes were incubated with a mouse monoclonal anti human β-actin and horseradish peroxidase-labelled goat anti-mouse Fab-fragments (Dianova), and visualized as described earlier. The films were scanned in order to perform a semiquantitative expression analysis using the Gel-Pro Analyzer software version 4.5.00.0 (Media Cybernetics Europe, Buckinghamshire, UK). The quantified signals were within the linear range in relation to the protein amount loaded onto the gel. OATP1B3 expression was normalized to the expression of β-actin. The expression of the mutants was calculated relative to the WT expression of OATP1B3 (WT expression = 1), and expressed as arbitrary units (a.u.). All samples were investigated at least in triplicates. Even though the purified antiserum showed some non-specific protein binding, the correct molecular size of OATP1B3 was detected as previously described (König *et al*., 2000).

For the OATP1B3 WT and the Lys41>Ala, Lys41>Gly, Arg580>Gly, Arg580>Lys and Glu77>Ala mutants, the cell

surface protein expression was investigated using the cell surface biotinylation technique with subsequent immunoblot analysis. The biotinylation and isolation of cell surface proteins were performed with the Pierce cell surface protein isolation kit (Thermo Scientific, Rockford, IL, USA) according to the manufacturer's instructions. Briefly, the cells were transfected as described earlier, and treated with the biotinylation reagent EZ-Link Sulfo-NHS-SS-Biotin (Thermo Scientific). Following cell lysis and solubilization of cell membranes, the protein amount of purified cell lysates was determined. The same protein amount was used for the isolation of OATP1B3 WT and mutants using NeutrAvidin agarose according to the manufacturer's instructions. The isolated OATP1B3 WT and mutants were analysed using immunoblot analyses as described earlier.

Transient transfection and uptake experiments

The transient transfection for the functional characterization of lysine and arginine mutants was performed as described for the immunofluorescence analysis. The uptake experiments were performed 24 h after the treatment of the cells with sodium butyrate. The uptake experiments using radiolabelled [^{3}H]BSP and non-radiolabelled pravastatin were performed as previously described (Seithel *et al.*, 2007; Bachmakov *et al.*, 2008). In brief, the cells were washed with pre-warmed (37°C) uptake buffer (142 mM NaCl, 5 mM KCl, 1 mM K_2HPO_4, 1.2 mM $MgSO_4$, 1.5 mM $CaCl_2$, 5 mM glucose and 12.5 mM HEPES, pH 7.3). Subsequently, the cells were incubated with 1 μM BSP (mixture of radiolabelled and non-radiolabelled BSP) or 50 μM pravastatin for 10 min at 37°C. The transport activity was in a linear range at this time-point. Subsequently, the cells were washed three times with ice-cold uptake buffer. The intracellular accumulation of radioactivity was measured using a liquid scintillation counter (Tricarb2800; PerkinElmer Life Sciences GmbH, Rodgau-Jügesheim, Germany) after the cells were lysed with 0.2% sodium dodecyl sulphate (SDS). The appropriate protein concentration of each well was determined by bicinchoninic acid assay (BCA Protein Assay Kit; Thermo Scientific). For pravastatin, the uptake assay was performed as described earlier except for the determination of the intracellular pravastatin accumulation. Following lysis of the cells with 0.2% SDS, the amount of intracellular pravastatin was determined by LC–MS/MS as previously described (Seithel *et al.*, 2007). All experiments were performed at least in triplicate. Michaelis–Menten-type non-linear curve fitting at 0.1, 0.5, 1.0, 5.0 and 10.0 μM BSP was performed to calculate the maximal uptake rate (V_{max}) and the concentration at which half of the maximal uptake occurs (K_m) using GraphPad Prism 4 (GraphPad Software, Inc., La Jolla, CA, USA). The obtained V_{max} values were normalized to the cell surface protein expression of the respective mutants. Transport rates are given in pmol (mg protein)$^{-1}$ min^{-1}.

Statistical analysis

All data are presented as mean ± SEM. The impact of the investigated mutants on the protein expression, transport activity and V_{max} was analysed using one-way ANOVA with Bonferroni's multiple comparison test. $P \leq 0.05$ was required for statistical significance. The calculations were performed using GraphPad Prism 4.

Materials

[^{3}H]Sulphobromophthalein ([^{3}H]BSP; 7585 GBq·mmol^{-1}) was obtained from Hartmann Analytic (Braunschweig, Germany). Unlabelled BSP and poly-D-lysine hydrobromide were purchased from Sigma-Aldrich Chemie GmbH (Taufkirchen, Germany). Pravastatin sodium salt was obtained from Tocris Cookson Inc. (Ellisville, MO, USA). Methanol (hypergrade quality) and sodium butyrate were purchased from Merck KGaA (Darmstadt, Germany). The polyclonal anti-human OATP1B3 antiserum (SKT3fr2) generated in a rabbit against the peptide sequence SKTCNLDMQDNAAAN was obtained from Peptide Specialty Laboratories GmbH (Heidelberg, Germany). The antiserum was further purified according to the supplier's instructions using a matrix with immobilized peptide. The cross reactivity of the purified antiserum against other human OATPs was tested performing an immunoblot analysis. No cross reactivity against the tested OATPs (OATP1B1, OATP2B1, OATP4A1, OATP4C1 and OATP5A1) was observed. All other chemicals and reagents, unless stated otherwise, were obtained from Carl Roth GmbH + Co. KG (Karlsruhe, Germany), and were of the highest grade available.

Structural modelling

Suitable templates for homology modelling were detected using the protein structure prediction server at the BioInfoBank Institute (Ginalski *et al.*, 2003). The individual prediction methods combined by the server consistently predicted that the glycerol-3-phosphate transporter (PDB code 1pw4; Huang *et al.*, 2003) and the lactose permease structure (PDB code 1pv6; Abramson *et al.*, 2003) share a significant structural similarity to OATP1B3. Modelling was performed based on these templates using Modeller 6.2 (Sanchez and Sali, 2000). Due to the limited sequence homology of the loop regions, modelling was restricted to the transmembrane helices. Hydrogen atoms were added to the final model, followed by 100 steps of conjugate gradient minimization using Sybyl7.3 (Tripos Inc., Munich, Germany). The quality of the structure was assessed using Procheck (Laskowski *et al.*, 1993) and Whatcheck (Hooft *et al.*, 1996). Finally, mutations were inserted using Sybyl7.3 and Swiss-PdbViewer (Guex and Peitsch, 1997), selecting the lowest-energy side chain conformer for each mutated residue.

Results

Alignment of human OATP family members and mutagenesis

A partial alignment of the amino acid sequences of all human OATP family members is shown in Figure 1. For the present study, the lysine residues at positions 28 and 41, and arginine at position 580 in OATP1B3 were chosen for further analyses. Lys28 and Lys41 are located in transmembrane helix I of OATP1B3, which faces the predicted pore of the transporter

(Meier-Abt *et al.*, 2005), and they are conserved in an additional seven and three human OATPs, respectively (Figure 1). Arginine 580 is conserved within all human OATPs and is predicted to be located in the pore-facing helix XI. Based on this alignment, we generated different OATP1B3 mutants. In detail, the residue lysine 28 was mutated to alanine (Lys28>Ala), arginine (Lys28>Arg; present in OATP5A1 and OATP6A1) and glycine (Lys28>Gly; present in OATP4C1). Lysine 41 was mutated to alanine (Lys41>Ala), arginine (Lys41>Arg), glutamine (Lys41>Gln; present in all other OATPs) and glycine (Lys41>Gly). The arginine 580 residue was mutated to alanine (Arg580>Ala), glycine (Arg580>Gly) and lysine (Arg580>Lys). Furthermore, a control mutant (Gly522>Cys) was generated, which has been analysed previously and which shows reduced BSP transport compared to the OATP1B3 WT (Letschert *et al.*, 2004). Because the structural modelling (Figure 7) revealed that the residue arginine 580 interacts with the adjacent residues glutamate 74 and asparagine 77, the additional single mutants Glu74>Ala and Asn77>Ala, and the double mutant Glu74>Ala_Asn77>Ala were generated.

Membrane localization of lysine and arginine mutants

In order to determine a possible influence of the respective lysine and arginine mutants on the membrane localization, immunofluorescence analyses were performed. As shown in Figure 2, no changes in the membrane localization were observed for the Lys28>Ala, Lys28>Arg, Lys28>Gly, Lys41>Ala, Lys41>Arg, Lys41>Gln, Lys41>Gly and Arg580>Gly mutants compared to the OATP1B3 WT. The control mutant Gly522>Cys did not also lead to a change in the membrane localization, which is in agreement with previously published data (Letschert *et al.*, 2004). Only for the Arg580>Ala and Arg580>Lys mutants, a minor intracellular retention of OATP1B3 in the cytoplasm and/or intracellular compartments was observed. A major amount of protein of these mutants was still detectable in the plasma membrane. Cells transfected with the empty vector (VC) did not show any positive staining of OATP1B3. Laser scanning of the *z*-dimension, which was performed in order to investigate the localization of the respective OATP1B3 proteins in the whole cell membrane, confirmed these results (Figure 2).

Protein expression and cell surface protein expression of OATP1B3 mutants

Figure 3 shows representative immunoblots of the investigated OATP1B3 mutants, the OATP1B3 WT, the control mutant Gly522>Cys and of the VC. The semiquantitative densitometric analysis revealed that the Arg580>Ala mutant

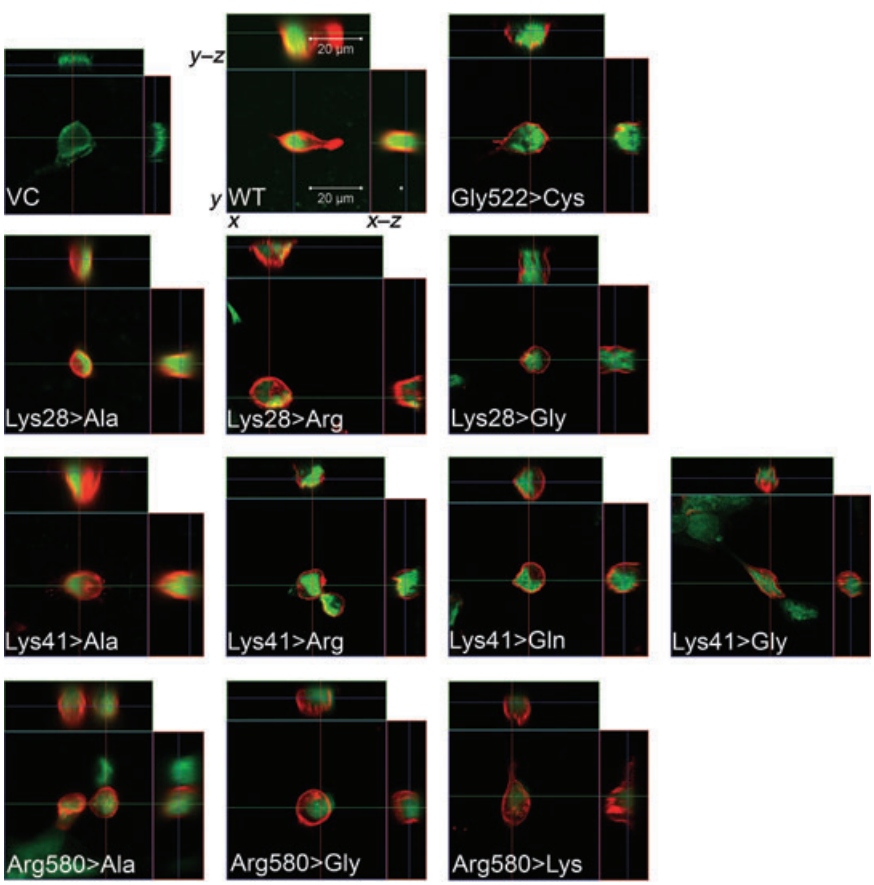

Figure 2 Immunofluorescence analysis by confocal microscopy of transiently transfected HEK293 cells expressing WT or mutant OATP1B3. VC: HEK293 cells transiently transfected with empty vector; WT: HEK293 cells transiently transfected with *SLCO1B3* WT. The other pictures show the different mutants (e.g. Lys28>Gly, lysine at position 28 was mutated to glycine). All investigated mutants showed a clear localization of the protein in the plasma membrane. Only for the Arg580>Lys and the Arg580>Ala mutants that a partial retention in the cytoplasm was observed. For each mutant, the *x–y*, *x–z* and *y–z* dimensions are shown. Red fluorescence, localization of OATP1B3; green fluorescence, nuclei staining.

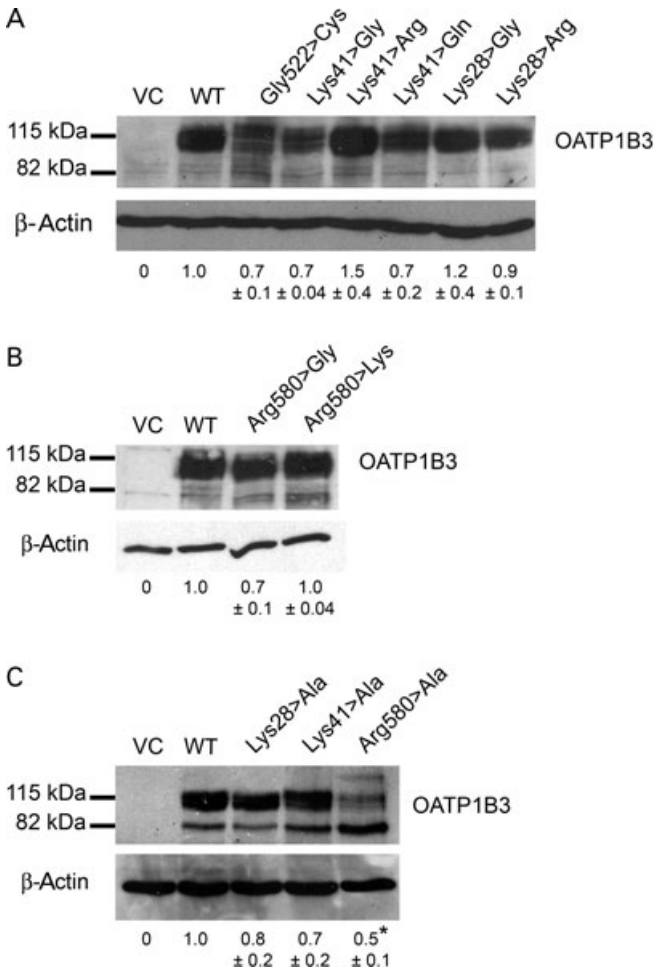

Figure 3 Representative immunoblot analysis of the OATP1B3 mutants at position Lys28, Lys41 and Arg580. The total OATP1B3 expression of the mutants Lys28, Lys41 and Arg580, and the control mutant Gly522>Cys compared to the WT and VC are shown. The results of densitometric analyses are given below. The data are expressed as mean ± SEM in arbitrary units (a.u.). No significant differences in the protein expression ($P > 0.05$) of the control mutant (Gly522>Cys) and the other mutants except for Arg580>Ala ($P < 0.05$) compared to OATP1B3 WT were observed (one-way ANOVA with Dunnett's multiple comparison test). (A) Mutants of Lys41 and Lys28; (B) mutants of Arg580; (C) mutants of Lys28, Lys41 and Arg580 to alanine. *$P < 0.05$; different from WT.

led to a significant reduction of total OATP1B3 expression (0.5 ± 0.1 a.u. compared to WT, $P < 0.05$). All other mutants of Lys28, Lys41 and Arg580 were characterized by no statistical significant differences of total OATP1B3 expression levels compared to WT (Figure 3).

For the OATP1B3 WT and the Lys41>Ala, Lys41>Gly, Arg580>Gly, Arg580>Lys and Glu77>Ala mutants, the cell surface protein expression was investigated in order to normalize the obtained V_{max} values to the cell surface protein expression. Figure 4 shows a representative immunoblot of the cell surface protein expression of the investigated OATP1B3 mutants and the WT. The Lys41>Ala and Lys41>Arg mutants were characterized by a 1.7- and 1.3-fold increase respectively. The Arg580>Gly, Arg580>Lys and Glu74>Ala mutants showed decreased surface expression (0.5-fold) compared to the WT.

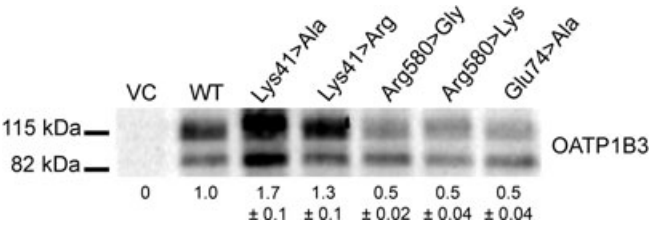

Figure 4 Representative immunoblot analyses of the cell surface protein expression of OATP1B3 mutants at positions Lys41, Arg580 and Glu74 compared to the WT and VC are shown. The results of densitometric analyses are given below. The data are expressed as mean ± SEM in arbitrary units (a.u.).

Influence of OATP1B3 mutants on the uptake of BSP and pravastatin

The effect of the lysine and arginine mutants on the cellular uptake of the OATP1B3 substrates BSP and pravastatin is shown in Figure 5. In all experiments, the control mutant Gly522>Cys showed a marked reduction in the OATP1B3-mediated uptake of BSP and pravastatin compared to OATP1B3 WT, which is in agreement with previously published data (Letschert *et al.*, 2004). The amino acid changes at position 28 (Lys28>Arg or Lys28>Gly) did not influence the cellular uptake of BSP, or that of pravastatin, relative to WT. As expected, the Lys41>Arg mutant revealed no decrease in the uptake of BSP and a non-significant decrease in pravastatin uptake, whereas the changes to an uncharged amino acid (Lys41>Gln or Lys41>Gly) showed a significantly reduced transport for BSP and pravastatin (all $P < 0.01$), relative to WT. This indicated that the positive charge of lysine, which is replaced by arginine, was pivotal for the uptake of both investigated substrates.

As expected, the Arg580>Gly mutant showed significantly reduced transport rates for BSP and pravastatin relative to WT (both $P < 0.01$). Interestingly, Arg580>Lys also showed a significant reduction of BSP and pravastatin transport ($P < 0.01$), suggesting that only arginine was able to mediate the transport of both substrates. The VC cells were characterized by low uptake of BSP and pravastatin, relative to WT (Figure 5). In order to confirm the results of the change to the neutral amino acid glycine for the BSP transport, the mutants Lys28>Ala and Lys41>Ala were also investigated regarding their BSP transport, and showed results (96 ± 2% and 15 ± 1%; $P < 0.01$, relative to WT, respectively) similar to those of the corresponding glycine mutants (Lys28>Gly, Lys41>Gly). Therefore, no further analyses of Lys28>Ala and Lys41>Ala for pravastatin uptake were performed. Arg580>Ala was excluded from all analyses due to the reduced protein expression (Figure 3).

Influence of OATP1B3 mutants on kinetic parameters of BSP uptake

We further determined the influence of positive charges on the kinetic parameters of BSP transport mediated by selected OATP1B3 mutants. Therefore, substrate-dependent transport studies of WT, Lys41>Ala, Lys41>Arg, Arg580>Gly and Arg580>Lys were performed. Figure 6 shows the results of kinetic analyses of the investigated OATP1B3 WT and the

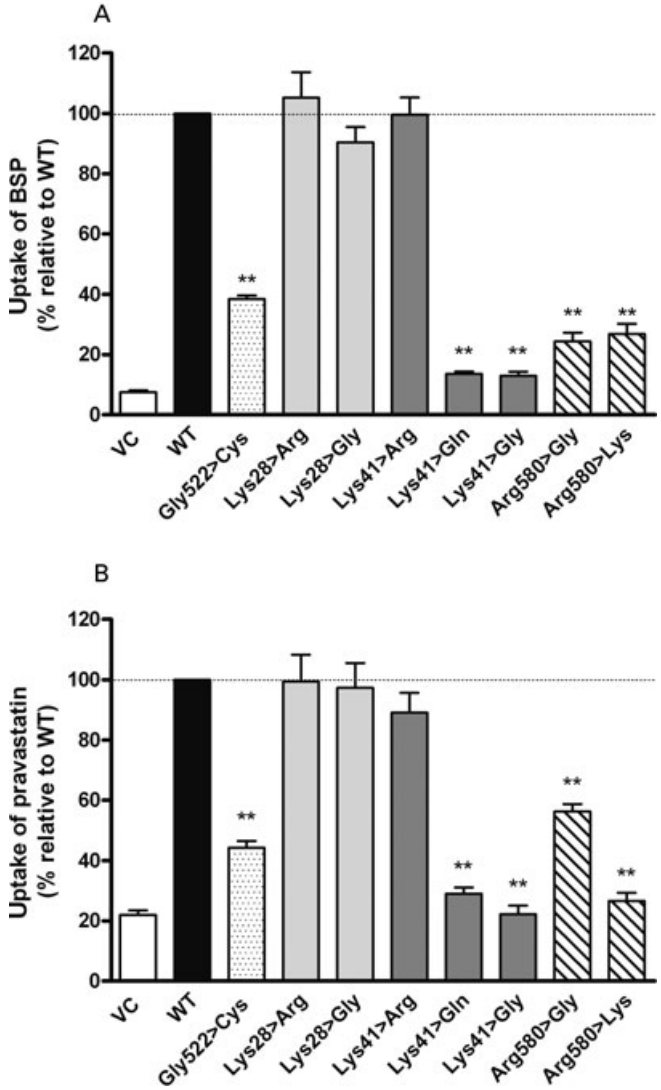

Figure 5 OATP1B3-mediated (A) BSP (1 μM) and (B) pravastatin (50 μM) uptake (10 min) by mutant OATP1B3 proteins compared to the WT and vector-transfected HEK293 cells (VCs). The transport activity is expressed in percent relative to the WT transport activity (100%). Data were analysed by ANOVA with Dunnett's multiple comparison test (compared to WT) was performed (**$P < 0.01$; different from WT). The Lys>Gln and Lys>Gly mutants at position 41 showed reduced transport activity for pravastatin and/or BSP, whereas Lys41>Arg rescued the transport activity. The Arg580>Gly and Arg580>Lys mutants were characterized by a reduced uptake activity.

respective mutants. The Lys41>Ala mutant was characterized by a non-significant change in K_m. The estimated V_{max} value, normalized to the cell surface protein expression was significantly reduced ($P < 0.001$), compared to the V_{max} value of the WT. In contrast, the Lys41>Arg mutant showed no difference in K_m or V_{max} ($P > 0.05$), relative to the WT. This confirmed that the positive charge at position 41 was pivotal for the transport activity. The reduced V_{max} value of Arg580>Gly (Figure 6) may suggest that the positive charge of Arg580 is important for the transport activity of OATP1B3. The replacement of arginine by lysine at position 580 resulted in a K_m value and a V_{max} (normalized to cell surface protein expression) of the Arg580>Lys mutant not different from those of the WT ($P > 0.05$; Figure 6), indicating that the positive charge of arginine can also be replaced by lysine.

Structural modelling

Our structural modelling of OATP1B3 revealed that lysine 28, which is located at the end of helix I, is not facing the pore because the helix is tilted with respect to the membrane (Figure 7A and B). Lysine 41 is oriented to the inside of the pore and does not form stabilizing interactions with adjacent amino acids (Figure 7A–C). This suggests that the lysine 41 side chain is flexible within the pore. When lysine is replaced by arginine at position 41, clashes were observed with residues (Tyr208) in helix V (Figure 7D). These clashes result from the longer arginine side chain compared to lysine, and are expected to reduce the flexibility of Arg41 and to favour an alternative side chain conformation. The alternative side chain conformation is additionally stabilized by a hydrogen bond with Ser37 (Figure 7E), which is expected to further reduce the flexibility of Arg41.

The side chain of Arg580 is predicted to be oriented to the inside of the pore. This orientation is stabilized by polar interactions with the side chains of glutamate 74 and asparagine 77 (Figure 7F). These interactions cannot be formed with the shorter side chain of lysine, which will result in an alternative orientation and/or increased flexibility of the lysine side chain (Figure 7G).

Characterization of Glu74>Ala and Asn77>Ala mutants

In order to investigate the relevance of the fixation of Arg580 by Glu74 and Asn77, the additional mutants Glu74>Ala, Asn77>Ala and Glu74>Ala_Asn77>Ala were generated. The membrane localization of these mutants showed no changes compared to WT (Figure 8A). The protein expression of Glu74>Ala was not significantly different compared to the WT, whereas the Asn77>Ala and Glu74>Ala_Asn77>Ala mutants were characterized by a significant decrease ($P < 0.01$) in protein amount (Figure 8B). The kinetic analysis of the Glu74>Ala mutant revealed a moderate decrease in V_{max} value normalized to the cell surface protein expression ($P > 0.05$), and a slight increase in K_m value (Figure 8C), indicating that Glu74 is involved to some extent in the transport process due to the interaction with Arg580. The Asn77>Ala and Glu74>Ala_Asn77>Ala mutants were excluded from this analysis due to their reduced protein levels.

Discussion

In this study, we investigated the role of the positively charged amino acids lysine 28 and 41, and of arginine 580 predicted to be located in pore-facing transmembrane helices of OATP1B3. Our major finding was that the positive charges of Lys41 and Arg580 in OATP1B3 are important for transport activity of the OATP1B3 substrates BSP and pravastatin.

The basis for our study was the structure-based modelling of the OATP1B3 protein by Meier-Abt *et al.* (2005). They suggested that OATP1B3 has a positively charged central pore

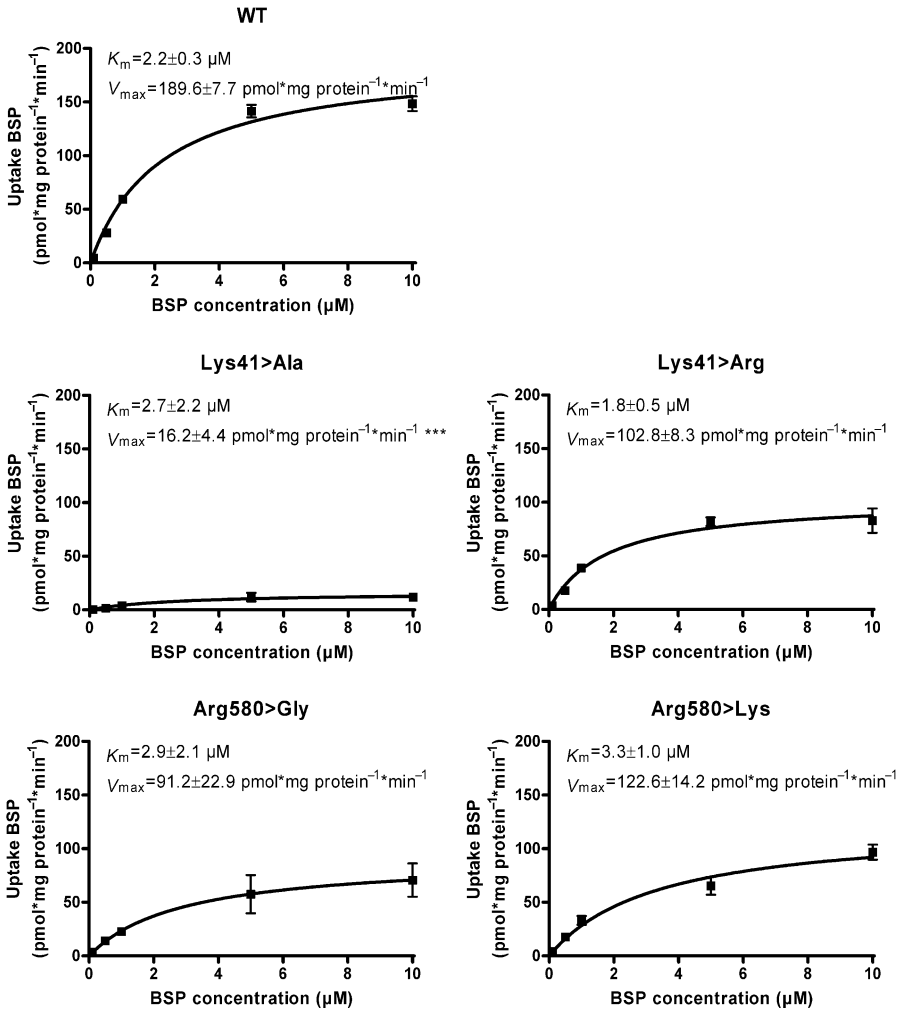

Figure 6 Michaelis–Menten kinetics of BSP net uptake mediated by OATP1B3 WT and the mutants Lys41>Ala, Lys41>Arg, Arg580>Gly and Arg580>Lys. The uptake of BSP was measured at 10 min. The V_{max} values are normalized to cell surface protein expression of OATP1B3 WT/mutants. Data are presented as mean ± SEM. ***Significantly different compared to WT, $P < 0.001$.

inside. Due to our alignment of all human OATP family members (Figure 1), we identified lysine residues at positions 28 and 41, as well as arginine at position 580, in OATP1B3 as potentially important candidates for the transport activity, because they are highly conserved among the human OATP family and these residues were predicted to be located in the pore-facing helices I and XI respectively (Meier-Abt *et al.*, 2005). Therefore, it was possible that these amino acids were important for substrate binding and transport activity within the OATP1 subfamily.

The OATP1B3-mediated uptake by the Lys41 mutants we generated demonstrated that the positive charge at position 41 of lysine is important for the cellular uptake of BSP and pravastatin, because substitution by the amino acids alanine, glutamine and glycine showed strongly reduced transport activity. Instead, the uptake was almost rescued by providing the positive charge from arginine. The moderately reduced V_{max} of Lys41>Arg compared to the WT indicates that the amino acid lysine is superior to arginine for transport activity. We speculated that the longer positively charged side chain of arginine leads to a reduced transport activity due to steric changes and interference. This was confirmed by structural modelling, which indicated that lysine 41 is flexible within the pore, whereas arginine at this position is predicted to have a reduced flexibility due to steric clashes and novel interactions with Ser37 and Tyr208, which stabilize an alternative side chain orientation (Figure 7D and E).

Kinetic analysis of Arg580 revealed that the change to the uncharged amino acid glycine resulted in a reduced V_{max}, confirming that the positive charge at position 580 is crucial for the transport activity. The substitution of Arg580 by lysine also led to a partial rescue of the V_{max} value of BSP uptake. Our structural modelling predicted that at position 580, only arginine is adequately fixed within the pore by interactions with the residues Glu74 and Asn77 (Figure 7F). In contrast, the modelling of the Arg580>Lys mutant predicted that lysine is not fixed because of the loss of interaction with Glu74 and Asn77. Additionally, the mutation of Glu74 to alanine caused a moderate decrease in V_{max}, which may indicate that this residue is relevant for the transport activity of OATP1B3. The results from the Glu74>Ala mutant were comparable to the results from the Arg580>Lys mutant, indicating that the

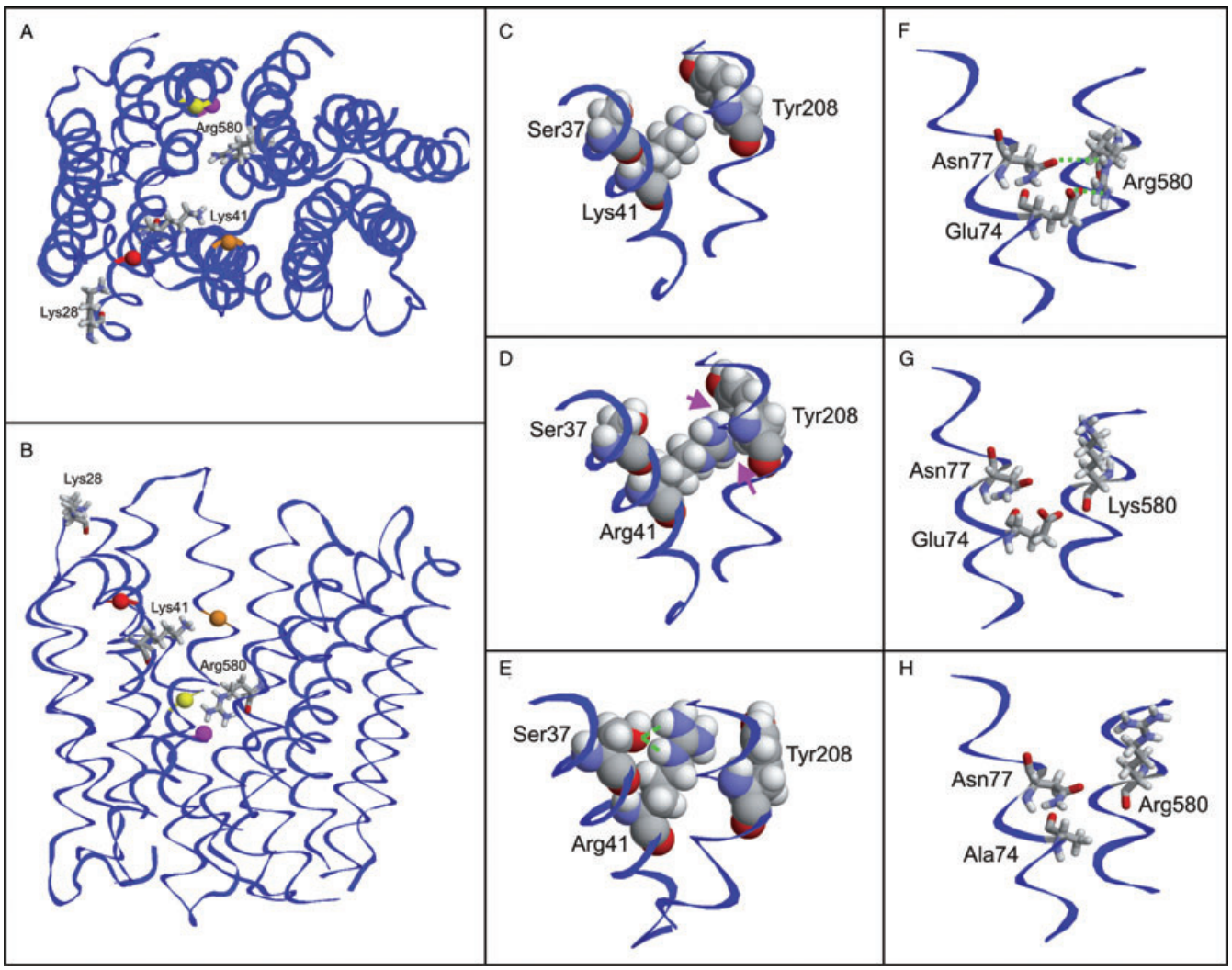

Figure 7 Structural modelling of OATP1B3. Top view (A) and side view (B) of the model showing the positions of the investigated residues. The positively charged amino acids are shown as stick presentation and are labelled. Adjacent amino acids, which are discussed in the text, are shown as balls and are colour coded as follows: Ser37 (red), Tyr208 (orange), Glu74 (magenta) and Asn77 (yellow). (C–E) Effect of the Lys41>Arg mutation: While the Lys41 side chain shows no interactions with adjacent amino acids (C), Arg41 exhibits minor clashes (D; magenta arrows), which probably lead to an alternative side chain conformation (E; green lines indicate an interaction with Ser37). (F–H) Effect of the Arg580>Lys and Glu74>Ala mutations: The orientation of Arg580 is stabilized by interactions with Glu74 and Asn77 (F), which cannot be formed by a lysine (G) resulting in an altered side chain orientation. The same loss of interactions is predicted for a Glu74>Ala mutation (H).

positive charge of Arg580 needs to be fixed within the pore, and alterations in this fixation influence the transport activity of OATP1B3. It should be noted that comparable kinetic results within the same range were caused either by the mutation of arginine 580 to lysine or by a mutation of the amino acid glutamate 74 to alanine, which is responsible for fixation of Arg580 according to our modelling. These data strongly suggest that the fixation of Arg580 by Glu74 and Asn77 is important for transport activity.

Mutants of Lys28 had no impact on the cellular uptake of BSP and pravastatin, indicating that the positive charge of Lys28 is not involved in substrate binding of both investigated substrates. This is in good agreement with our structural model showing that lysine 28 is located at the end of helix I and is not facing the pore (Figure 7A and B).

Our experimental data and structural modelling strongly indicate that the positive charges of lysine 41 and arginine 580 are lining the pore. Moreover, due to particular structural requirements, both residues cannot be replaced by another positively charged amino acid without influencing transport activity.

Lysine 41 is conserved within the OATP1 subfamily, whereas arginine 580 is conserved within all human OATPs (Figure 1), suggesting that these amino acids might play a pivotal role in formation of the positively charged pore. In addition, the strict conservation might additionally be important for larger-scale structural changes during the transport process, which cannot be deduced from the present static model.

For pravastatin, it can be concluded that Lys41 and Arg580 are also relevant for the OATP1B3-mediated uptake. However, the effect of investigated mutants on the K_m and V_{max} values of the OATP1B3-mediated transport of pravastatin might be different because it is possible that pravastatin is transported by

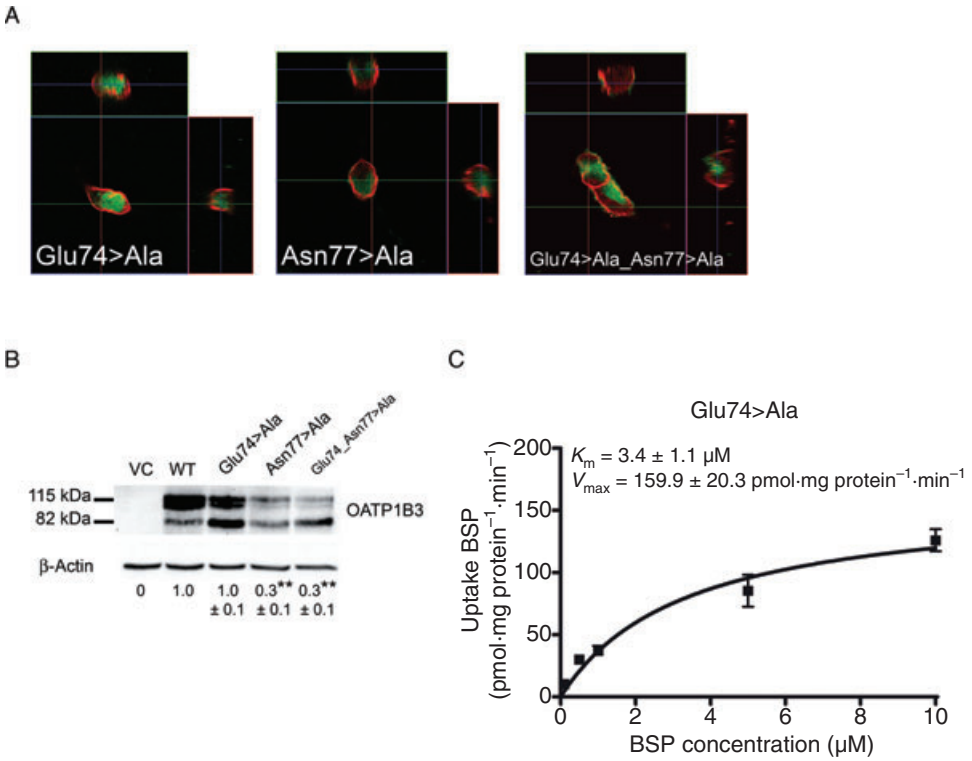

Figure 8 Characterization of the Glu74>Ala, Asn77>Ala and Glu74>Ala_Asn77>Ala mutants. Immunofluorescence (A), immunoblot analysis (B) of all mutants are shown. $^{**}P < 0.01$, different from WT. In (C) Michaelis–Menten kinetics of the Glu74>Ala mutant are shown. The uptake of BSP mediated by Glu74>Ala was measured at 10 min. The V_{max} value is normalized to cell surface protein expression of Glu74>Ala. The Asn77>Ala and Glu74>Ala_Asn77>Ala mutants showed decreased protein expression (see B) and were therefore excluded from kinetic analysis.

a different mechanism. Evidence for different OATP1B3-mediated transport mechanisms of BSP and pravastatin was obtained from a study which showed that 10 µM rosiglitazone inhibited the BSP uptake, whereas the same rosiglitazone concentration stimulated the uptake of pravastatin (Bachmakov *et al.*, 2008).

Interestingly, a recent study by Gui and Hagenbuch (2008) demonstrated that uncharged polar amino acids such as tyrosine, serine and threonine residues located in the transmembrane domain X of OATP1B3 are also involved in the transport of the OATP1B3-specific substrate cholecystokinin octapeptide (CCK-8). In combination with our data, it can be concluded that in addition to positively charged amino acids, uncharged non-polar amino acids could also be important for the transport mechanism of OATP1B3 maybe by interacting with positively charged residues.

Taken together, we provide the first experimental evidence for the involvement of conserved positively charged amino acids in the transport of OATP1B3. Our findings are supported by our structural modelling, and the proposed concept of a positively charged pore in OATPs by Meier-Abt *et al.* (2005). We were able to demonstrate that the amino acids lysine 41 and arginine 580 in OATP1B3, which are conserved within the human OATP family, are important and crucial for OATP1B3-mediated transport of substrates such as BSP.

Acknowledgements

We are very grateful for the technical assistance of Daniel Auge, Krystyna Bujok, Claudia Hoffmann, Marion Rittmaier and Ingrid Schmidt. This work was supported by the grants of Deutsche Forschungsgemeinschaft (DFG KO 2120/1-3 and DFG GL 588/2-1), and a grant from the Deutsche Krebshilfe (107854).

Conflict of interest

All authors declare no conflict of interest.

References

Abe T, Unno M, Onogawa T, Tokui T, Kondo TN, Nakagomi R *et al.* (2001). LST-2, a human liver-specific organic anion transporter, determines methotrexate sensitivity in gastrointestinal cancers. *Gastroenterology* **120** (7): 1689–1699.

Abramson J, Smirnova I, Kasho V, Verner G, Kaback HR, Iwata S (2003). Structure and mechanism of the lactose permease of *Escherichia coli*. *Science* **301** (5633): 610–615.

Bachmakov I, Glaeser H, Fromm MF, König J (2008). Interaction of oral antidiabetic drugs with hepatic uptake transporters: focus on organic anion transporting polypeptides and organic cation transporter 1. *Diabetes* **57** (6): 1463–1469.

Cui Y, König J, Buchholz JK, Spring H, Leier I, Keppler D (1999). Drug resistance and ATP-dependent conjugate transport mediated by the apical multidrug resistance protein, MRP2, permanently expressed in human and canine cells. *Mol Pharmacol* **55** (5): 929–937.

Cui Y, König J, Keppler D (2001). Vectorial transport by double-transfected cells expressing the human uptake transporter SLC21A8 and the apical export pump ABCC2. *Mol Pharmacol* **60** (5): 934–943.

Devereux J, Haeberli P, Smithies O (1984). A comprehensive set of sequence analysis programs for the VAX. *Nucleic Acids Res* **12** (1 Pt 1): 387–395.

Ginalski K, Elofsson A, Fischer D, Rychlewski L (2003). 3D-Jury: a simple approach to improve protein structure predictions. *Bioinformatics* **19** (8): 1015–1018.

Glaeser H, Fromm MF (2008). Animal models and intestinal drug transport. *Expert Opin Drug Metab Toxicol* **4** (4): 347–361.

Glaeser H, Drescher S, van der Kuip H, Behrens C, Geick A, Burk O *et al*. (2002). Shed human enterocytes as a tool for the study of expression and function of intestinal drug-metabolizing enzymes and transporters. *Clin Pharmacol Ther* **71** (3): 131–140.

Glaeser H, Bailey DG, Dresser GK, Gregor JC, Schwarz UI, McGrath JS *et al*. (2007). Intestinal drug transporter expression and the impact of grapefruit juice in humans. *Clin Pharmacol Ther* **81** (3): 362–370.

Gradhand U, Tegude H, Burk O, Eichelbaum M, Fromm MF, König J (2007). Functional analysis of the polymorphism-211C>T in the regulatory region of the human *ABCC3* gene. *Life Sci* **80** (16): 1490–1494.

Guex N, Peitsch MC (1997). SWISS-MODEL and the Swiss-PdbViewer: an environment for comparative protein modeling. *Electrophoresis* **18** (15): 2714–2723.

Gui C, Hagenbuch B (2008). Amino acid residues in transmembrane domain 10 of organic anion transporting polypeptide 1B3 are critical for cholecystokinin octapeptide transport. *Biochemistry* **47** (35): 9090–9097.

Hagenbuch B, Meier PJ (2003). The superfamily of organic anion transporting polypeptides. *Biochim Biophys Acta* **1609** (1): 1–18.

Hagenbuch B, Meier PJ (2004). Organic anion transporting polypeptides of the OATP/SLC21 family: phylogenetic classification as OATP/SLCO superfamily, new nomenclature and molecular/functional properties. *Pflugers Arch* **447** (5): 653–665.

Hänggi E, Grundschober AF, Leuthold S, Meier PJ, St-Pierre MV (2006). Functional analysis of the extracellular cysteine residues in the human organic anion transporting polypeptide, OATP2B1. *Mol Pharmacol* **70** (3): 806–817.

Ho RH, Tirona RG, Leake BF, Glaeser H, Lee W, Lemke CJ *et al*. (2006). Drug and bile acid transporters in rosuvastatin hepatic uptake: function, expression and pharmacogenetics. *Gastroenterology* **130** (6): 1793–1806.

Hooft RW, Vriend G, Sander C, Abola EE (1996). Errors in protein structures. *Nature* **381** (6580): 272.

Huang Y, Lemieux MJ, Song J, Auer M, Wang DN (2003). Structure and mechanism of the glycerol-3-phosphate transporter from *Escherichia coli*. *Science* **301** (5633): 616–620.

König J, Cui Y, Nies AT, Keppler D (2000). Localization and genomic organization of a new hepatocellular organic anion transporting polypeptide. *J Biol Chem* **275** (30): 23161–23168.

Kullak-Ublick GA, Ismair MG, Stieger B, Landmann L, Huber R, Pizzagalli F *et al*. (2001). Organic anion-transporting polypeptide B (OATP-B) and its functional comparison with three other OATPs of human liver. *Gastroenterology* **120** (2): 525–533.

Laskowski RA, Moss DS, Thornton JM (1993). Main-chain bond lengths and bond angles in protein structures. *J Mol Biol* **231** (4): 1049–1067.

Lee W, Glaeser H, Smith LH, Roberts RL, Moeckel GW, Gervasini G *et al*. (2005). Polymorphisms in human organic anion-transporting polypeptide 1A2 (OATP1A2): implications for altered drug disposition and central nervous system drug entry. *J Biol Chem* **280** (10): 9610–9617.

Letschert K, Keppler D, König J (2004). Mutations in the *SLCO1B3* gene affecting the substrate specificity of the hepatocellular uptake transporter OATP1B3 (OATP8). *Pharmacogenetics* **14** (7): 441–452.

Meier-Abt F, Mokrab Y, Mizuguchi K (2005). Organic anion transporting polypeptides of the OATP/SLCO superfamily: identification of new members in nonmammalian species, comparative modeling and a potential transport mode. *J Membr Biol* **208** (3): 213–227.

Nozawa T, Sugiura S, Nakajima M, Goto A, Yokoi T, Nezu J *et al*. (2004). Involvement of organic anion transporting polypeptides in the transport of troglitazone sulfate: implications for understanding troglitazone hepatotoxicity. *Drug Metab Dispos* **32** (3): 291–294.

Sanchez R, Sali A (2000). Comparative protein structure modeling. Introduction and practical examples with modeller. *Methods Mol Biol* **143**: 97–129.

Seithel A, Eberl S, Singer K, Auge D, Heinkele G, Wolf NB *et al*. (2007). The influence of macrolide antibiotics on the uptake of organic anions and drugs mediated by OATP1B1 and OATP1B3. *Drug Metab Dispos* **35** (5): 779–786.

Senger M, Glatting KH, Ritter O, Suhai S (1995). X-HUSAR, an X-based graphical interface for the analysis of genomic sequences. *Comput Methods Programs Biomed* **46** (2): 131–141.